PHOENICS´ Applications in the Aluminium Smelting Industry

Ch. Droste

VAW Aluminium-Technologie GmbH

53117 Bonn, Germany

The multi-phase fluid system in aluminium reduction cells is exposed to strong electromagnetic forces which give rise to various steady-state and transient physical phenomena. The mastering and control of these magnetohydrodynamic (MHD) effects is one of the key factors for the successful operation of the reduction process with high current efficiency and low power consumption.

Based on the ESTER/PHOENICS ground code invented by CHAM, a detailed three-dimensional model of a reduction cell including the anode/cathode configuration, the electrolytic bath, the molten metal and ledge profile was set up. The fully coupled iterative solution of the magnetohydrodynamic equations in the fluid region and the electromagnetic field equations in the anodes/cathodes take into consideration the alteration and redistribution of the electrical and magnetic fields due to the movement of the molten metal and the metal pad deformation. Steady-state as well as transient cases can be investigated. The ESTER code is fully integrated with other process modelling tools. A preprocessor generates the input files from a common data base and a postprocessor prepares the results for visualization and extracts the characteristic quantities.

The MHD model is intensively used as a standard tool for formulating the layout of new reduction cell designs and for improving existing cells. Furthermore, it allows the thorough analysis of special operating conditions and the optimization of operational parameters.

Introduction

Aluminium is produced commercially by electrolytical reduction of aluminium oxide (Al_2O_3), solved in molten cryolite (Na_3AlF_6). Nowadays the development of the basic technology for the reduction process, named after its inventors Hall-Heroult process, is heavily based on numerical simulation tools [8]. These methods, based on scientific principles allow the realistic prediction of cell performance with respect to the key criteria. Most of the relevant physical aspects of the Hall-Heroult process are modelled in detail. In general, the
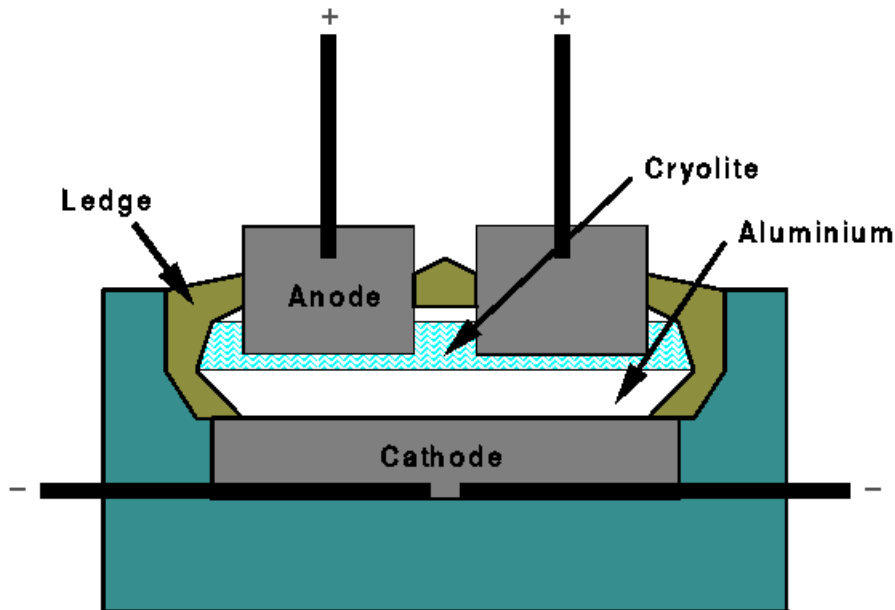
Figure 1: Cross-section of a alumina reduction cell – schematic drawing

mathematical models have to deal with two essential topics, namely thermoelectrics and magnetohydrodynamics. For the numerical simulation of the magnetohydrodynamics of the Hall-Heroult process CHAM introduced in 1982 an add-on to PHOENICS called ESTER, which stands for Electrolytic Smelter, c.f. [1]. The code was completely rewritten for PHOENICS 1.4 in 1987.

Especially for the prediction of steady-state phenomena ESTER has proven to be a valuable tool. For several years an extension of ESTER is part of VAW Aluminium-Technologies simulation package for the elaboration of concepts for improving cell performance [8]. Results of a steady-state ESTER simulation are presented.

ESTER has also been applied to the simulation of interfacial waves in reduction cells, c. f. [2, 3, 4]. But the significance of these results for improving cell performance was minor. A much better understanding of the mechanisms generating MHD instabilities, accompanied by interfacial waves, could be gained from a linear stability analysis [5,6] instead of a *brute force* solution of the time dependent Navier-Stokes equations. It could be shown that to first order the occurrence of MHD instabilities does not depend on nonlinear convection phenomena.

Promising is a combined application of ESTER and the linear MHD stability. The coupling of both methods was used to optimise the operation of a reduction cell [7]. The basic ideas with emphasis on the involved ESTER simulations are explained.
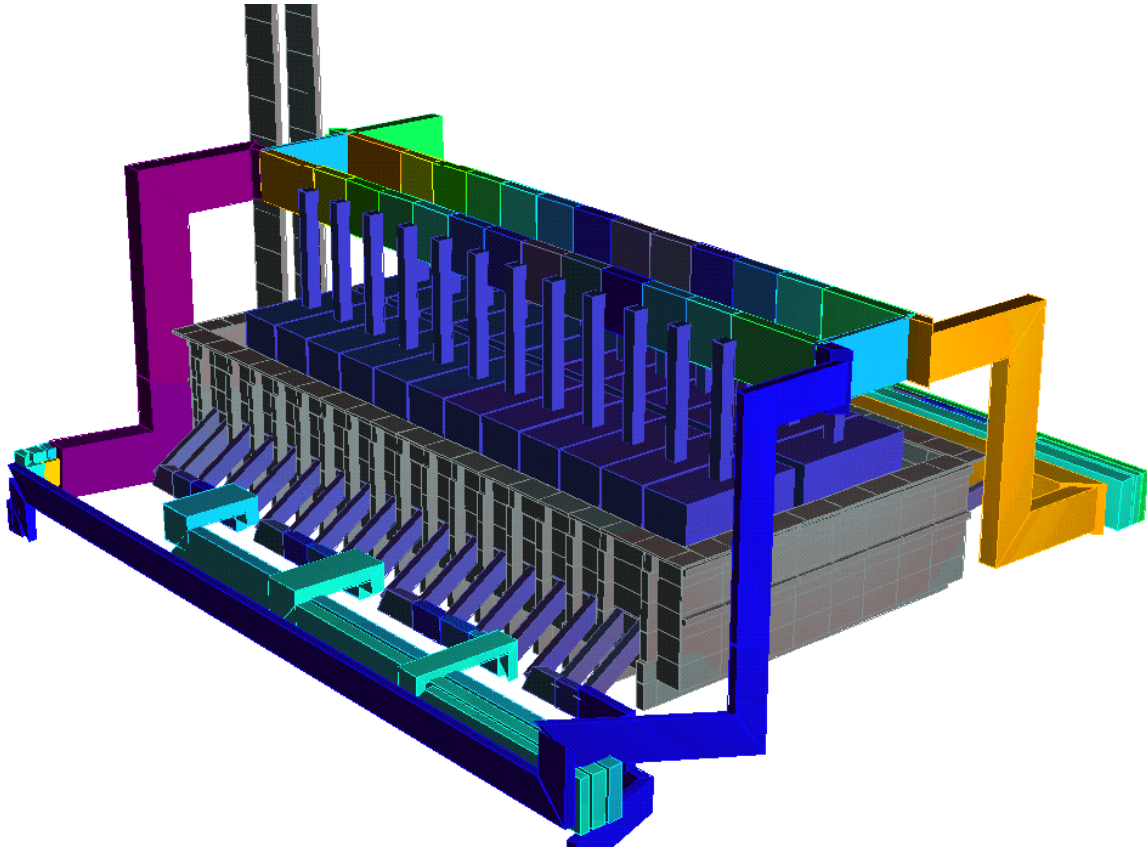
Figure 2: Simulation model of a reduction cell

Physical phenomena and mathematical description

The construction principle of a electrolytic cell is shown schematically in Fig. 1. Two liquid layers, the molten metal and the electrolyte (bath) floating on top of the metal are enclosed in a steel shell. The bottom is built by preformed carbon cathodes and insulating lining material. The side of the cell are covered by a ledge of frozen electrolyte. Carbon anodes are dipped into the electrolyte. Aluminium oxide (alumina) is feed to the electrolyte at regularly time intervals. The oxygen ions of the solved alumina are discharged electrolytically at the anodes accompanied by consumption of the anode carbon and generation of CO_2. The aluminium, formed at the metal/bath interface, accumulates at the bottom from where it is tapped periodically. The surface of the molten metal acts as the cathode. The metal height is in the range of 15-25 cm, the height of the electrolyte layer beneath the anodes (anode-cathode distance) is of the order of 5 cm.

For the reduction process a D.C. current of several 100,000 A is used. On the way form the anodes to the cathodes the current crosses both liquid layers. Around 50 % of the energy

input is used for decomposing of alumina and 50 % for maintaining the process temperature of 950-970 °C by Joule heating. Multiple anodes and cathodes are arranged in a cell. Depending on the plant layout 150-250 cells are connected in series. The current from one cell to the other is conducted via aluminium busbars. A simulation model of a reduction cell including busbars is shown in Fig. 2.

The electrical currents of the external busbars as well as the current in the cell are accompanied by strong magnetic fields. Electromagnetic forces (*Lorentz forces*) arise from the interaction between magnetic fields and the current distribution in the cell. Due to the low electrical conductivity of the bath and the high electrical conductivity of the molten metal there is a jump of the electrical field at the metal/bath interface. Whereas the current in the bath is mainly vertical directed, additional horizontal currents appear in the metal layer. This results in a discontinuity of the forces at the metal/bath interface.

The *Lorentz forces* cause the following steady-state and transient MHD phenomena in reduction cells:

- Steady-State fluid flow of the electrolyte
- Steady-State fluid flow of the molten metal
- Steady-State deformation of the metal/bath interface
- Different types of MHD Instabilities, i. e. interfacial waves

Whereas the steady-state phenomena are always present, MHD instabilities occur in some special situations, e. g. after anode change or metal tapping. High MHD-stability, moderate metal and bath velocities, a feasible flow pattern, low vertical velocity gradients between molten metal and bath and a flat metal/bath interface are the secrets of good cell performance with a high current efficiency and a low energy consumption. By optimising the magnetic fields with the aid of a particular arrangement of the busbars these conditions can be achieved to a certain amount.

The most relevant aspects for the simulation of the MHD phenomena described above are included in ESTER:

- 3-D reduction cell geometry
- two layered liquids
- free surface flow (unknown interface contour)

- simultaneous solution of the constitutive equations for fluid flow and electrical current distribution

The full 3D geometry including the two liquids, the side ledge and the anode configuration is approximated in Cartesian co-ordinates. The anodes and the side ledge are modelled by volume porosities. The fluid motion for each liquid layer is described by the *Navier-Stokes* equation

$$\rho \frac{\partial \vec{u}}{\partial t} + \rho(\vec{u}\nabla)\vec{u} = -\nabla P + \mu \Delta \vec{u} + \rho \vec{g} + \vec{F}$$

including the *Lorentz force*

$$\vec{F} = \vec{j} x \vec{B}$$

resulting from the electrical current density $\vec{j}$ and the magnetic induction $\vec{B}$.

A floating grid in combine with an interface tracking method is used to determine the sharp interface between the bath and the molten metal from the condition of no net momentum-flux across the metal/bath interface.

The current distribution in the cell itself depends on the motion of the metal and of the shape of the metal/bath interface. The motion of the liquid metal in the presence of a magnetic field generates induced currents whereas the metal/bath interface determines the precise distribution of the electrical resistivity σ in the cell. The *Poisson* equation is solved

$$\nabla(\sigma\nabla\zeta) = S$$

for the electric potential ζ in the cell and hence for the electric current distribution $\vec{j}$. This potential equation is derived from the *Maxwell equations* under the assumption of *Ohm's law*

$$\vec{j} = -\sigma\nabla\zeta + \sigma\vec{u} \times \vec{B}$$

including induced currents (Faraday's law)

$$\vec{j}_{ind} = \sigma\vec{u} \times \vec{B}$$

which define the source

$$S = \nabla(\sigma \vec{u} \times \vec{B})$$

of the *Poisson* equation.

The magnetic fields due to the induced currents $\vec{j}_{ind}$ are not taken into account in the original ESTER code.

It is obvious that fluid flow and electrical current distribution depend in a rather complex way on each other. Both effects have to be solved self-consistently. The effects of temperature gradients in the fluids (buoyancy) are neglected because in general they are small. Thermal phenomena, however, are included in this model via the geometry of the side ledge of frozen bath as geometric boundary for the solution domain. An option to take into account gas-driven phenomena is also implemented in ESTER.

Modifications and Extensions of ESTER

In general the original ESTER code underestimates the occurring velocities. We traced this problem back to the treatment of the boundary conditions at blocked cells (anodes, side ledge). The results were improved by modifying the convection as well as the diffusion coefficients across fluid and blocked regions in Ground, group 8.8 and 8.9.

A major shortcoming of ESTER is, that it does not allow for the specification of individual anode currents. As already mentioned the anodes are consumables. Normally one anode is replaced each day. Because the current pick-up of a new set anode is rather slow, the anode current distribution can be very irregular. We therefore have modified the treatment of the potential equation in the anode region. As an additional input option an anode current distribution can now be passed to ESTER. In a similar manner the solution domain for the electrical potential equation was extended with regard to the cathode configuration.

Also an option for recalculation of the magnetic field was added. The algorithm, based on the law of *Biot-Savart*, calculates the update to the magnetic fields due to the deviations between the initially guessed current distribution (on which the magnetic field that is used as input is based on) and the appearing current distribution. This option is used in cases where strong inhomogeneous currents are expected.
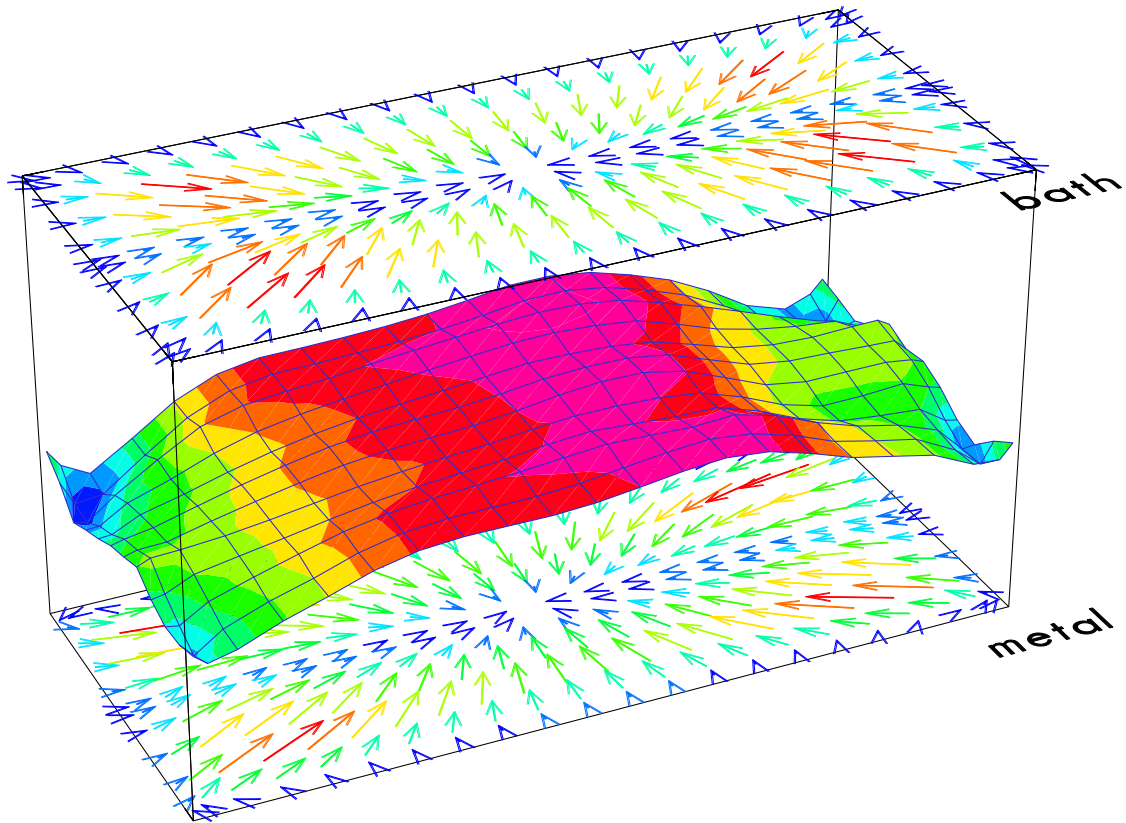
Figure 3: Lorentz forces in the metal and bath, pressure distribution across metal/bath interface

Applications

In the framework of the simulation tools of VAW Aluminium-Technology, the basic steps in analysing the MHD properties of a reduction cell are as follows [8]:

- Setting up of the geometry
- Network analysis for determination of the current distribution in the busbars
- Calculation of the magnetic field including ferromagnetic steel parts
- Steady-state MHD simulation of the liquids in the cell using ESTER
- MHD-Stability analysis by linear methods

All the calculations are done on the basis of a single input file. The essence of the input file is a parametric description of the cell geometry. Control parameters and material properties are also specified in this file. The input data for the different programs are deduced automatically
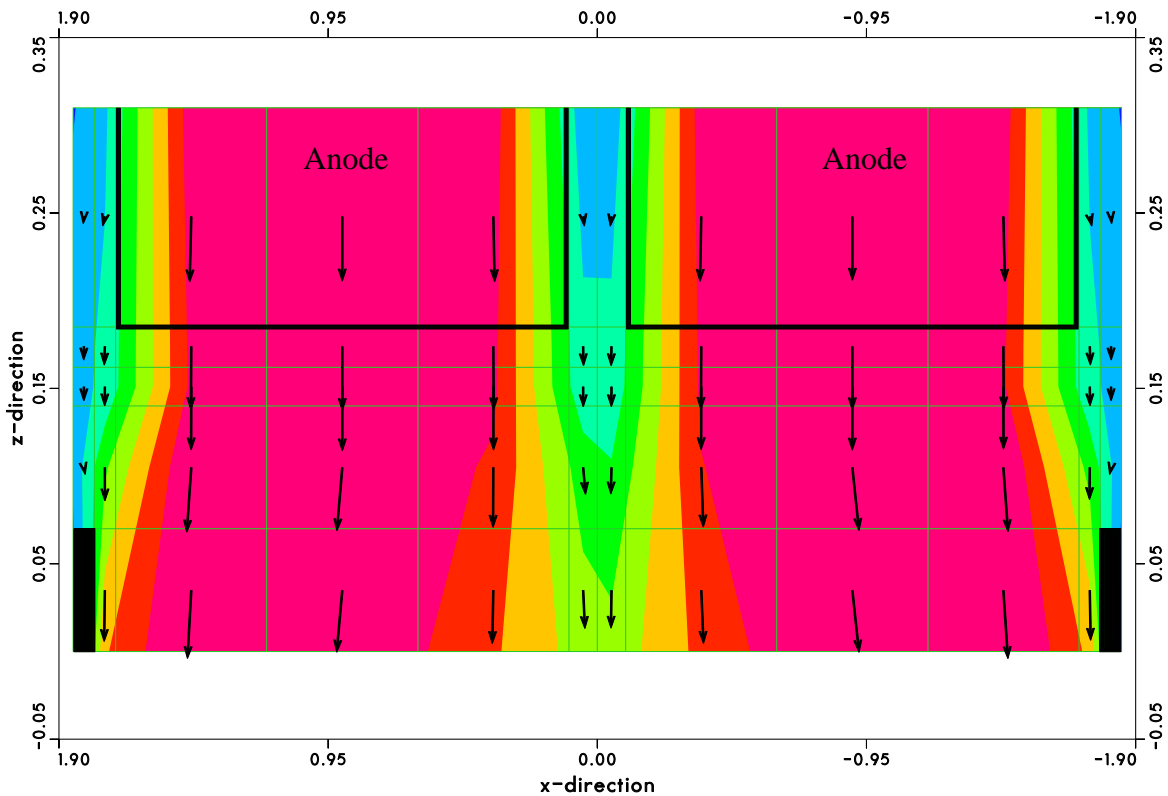
Figure 4: Electrical potential and electrical current density - sectional view

form this configuration file. From the configuration file and the result of the magnetic field calculation a pre-processor generates the q1 file for ESTER together with different input files which specify the boundary conditions. If required a pre-processor derives boundary conditions for the MHD-Stability analysis from the ESTER run.

This data organisation guaranties consistency between the different simulations and allows the investigation of a huge number of variants on the search for the optimum magnetic field.

For illustrating a typical steady-state magnetohydrodynamic simulation, ESTER was applied to a 170 kA reduction cell. As a result of the calculation Fig. 3 shows the *Lorentz forces* in the molten metal and electrolyte and in between the pressure difference across the metal/bath interface. The maximum forces are of the order of 100 N. Differences of the force fields in the metal and bath resulting from differences in the current distributions can be observed. The electrical potential and the belonging electrical current density for a cross-section of the cell is given in Fig. 4. The force fields and the pressure distribution give rise to the velocity pattern of the metal and bath and of the metal/bath interface contour displayed in
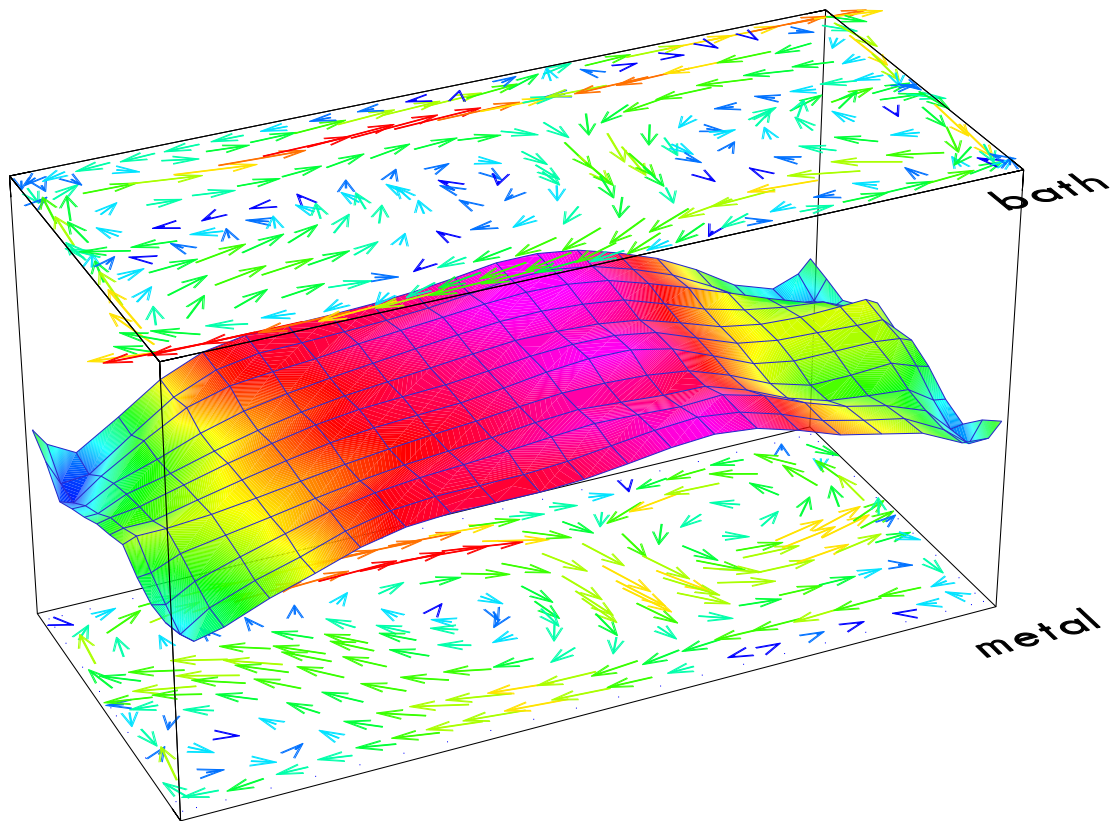
Figure 5: Flow field in the metal and bath and metal/bath interface contour

Fig 5. The flow field in the metal as well as in the bath is dominated by two eddies. Some smaller eddies occur at the boundaries. The mean velocities are about 8 cm/sec, the maximum speed goes up to 20 cm/sec. The metal pad heaving is around 5 cm.

The calculation takes just a few minutes on our computing environment. For convergence no more than 700 sweeps are necessary.

The next example demonstrates a more sophisticated application. It is part of a project for optimisation of an anode set pattern [7]. The replacement of spent anodes is one of the most disturbing operation for the reduction process. Often MHD instabilities occur just after the setting of a new anode. In general it takes several hours or even days until a new set anode has the full current load. At the moment when the next anode is changed the previous changed anode has not yet the full current pick-up. If the newly changed anodes are close together one can therefore expect a more severe disturbance to the magnetohydrodynamics of the cell. For that reason it is important to find an anode set pattern that gives on average the lowest disturbance to the cell. As a measure the tendency to build up MHD instabilities was analysed. The input for the MHD stability analysis namely the anode-cathode distribution

(the distance between metal surface and anode bottom) just after anode changing was derived from ESTER calculations.

For a complete anode set cycle the distribution of the anode-cathode distance and the flow field pattern is shown in Fig 6. For each anode change the following calculations were done:

- Steady-state simulation just before the anode change
- Steady-state simulation just after the insertion of the new anode

For the first run the burn-off flag of the ESTER input was activated. This option effects that all the anodes have the same distances to the metal surface. After a certain time of operation the shape of the anode bottoms follow the shape of the metal/bath interface due to the self-regulating mechanism of anode carbon consumption and anode current pick-up. The anode currents were set according to their individual age.

The second calculation restarts from the steady-state of the first run but with a deactivated anode burn-off flag. This means that now the heights of all anodes are fixed. This reflects the situation just after the anode change.

For the new set anode a nominal current of 10 % was assumed. As a consequence a complete redistribution of the currents takes place accompanied by a change of the metal/bath interface and the fluid flow. The redistribution of the anode-cathode distribution and the changed flow field for one possible anode set is shown in Figure 7. On the search for the optimum anode set pattern a huge number of such calculations have to be done.

Conclusion

The examples demonstrate that ESTER is a well suited basis for the simulation of the MHD phenomena in reduction cells. By additional ground coding ESTER can be adapted for special needs.

For steady-state applications good convergence is in general achieved and the results do not depend sensitively on the grid size. This together with a pre- and post-processing software for generating the input and preparing the output enables the use of ESTER as a
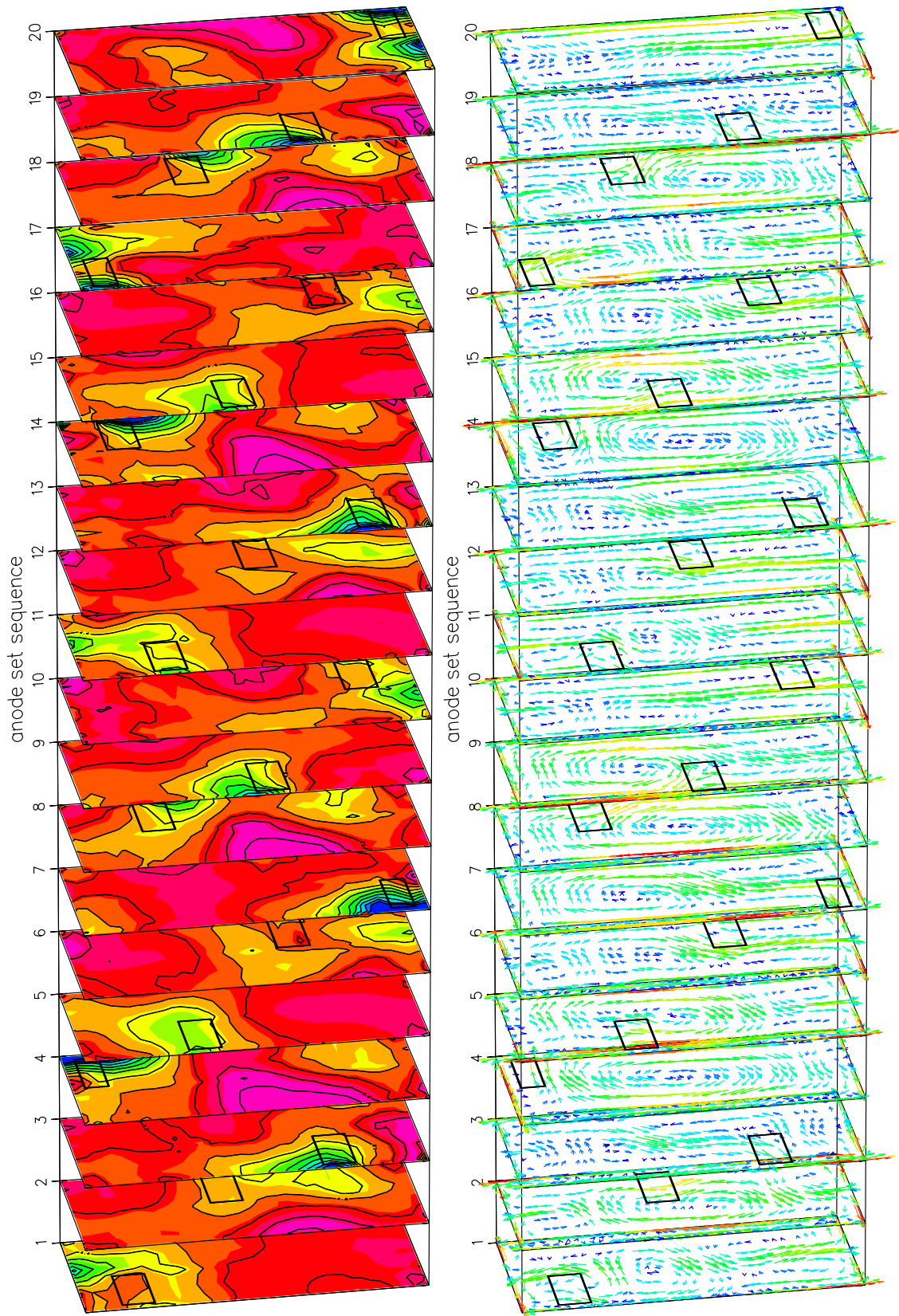
Figure 6: Anode-cathode distance distribution and fluid flow in the metal during a complete anode set cycle (rectangles indicate position of the new anode)

industrial design tool. Due to the low turn-around time of each calculation a huge number of variants can be investigated on the search for the optimal solution.

For the future there is potential for further improvements of ESTER concerning transient calculations and the gas-flow option. Also the analysis of MHD stability including convective phenomena should be feasible on the basis of ESTER.

References

[1] H. I. Rosten, The Mathematical Foundation of the ESTER Computer Code. CHAM TR/84, 1982.

[2] W. E. Wahnsiedler, Hydrodynamic Modeling of Commercial Hall-Heroult Cells. Light Metals 1987, pp. 269-287.

[3] V. Potocnik, Modeling of Metal-Bath Interface Waves in Hall-Heroult Cells using ESTER/PHOENICS. Light Metals 1989, pp. 227-235.

[4] M. Segatz, D. Vogelsang, Ch. Droste and P. Baekler, Modeling of Transient Magneto-Hydrodynamic Phenomena in Hall-Heroult Cells. Light Metals 1993, pp. 361-368.

[5] M. Segatz and Ch. Droste, Analysis of Magnetohydrodynamic Instabilities in Aluminium Reduction Cells. Light Metals 1994, pp. 313-322

[6] Ch. Droste, M. Segatz and D. Vogelsang, Improved 2-Dimensional Model for Magnetohydrodynamic Stability Analysis in Reduction Cells. Light Metals 1998, pp. 419-428

[7] M. Segatz, Ch. Droste and D. Vogelsang, Magnetohydrodynamic Effect of Anode Set Pattern on Cell Performance. Light Metals 1997, pp. 429-435

[8] D. Vogelsang, Application of Process Modelling to Improve Aluminium Production. Proc. 6th Aust. Al. Smelting Workshop 1998, pp. 211-225